The flow of swirling water through a convergent–divergent nozzle

By A. M. BINNIE, G. A. HOOKINGS* and M. Y. M. KAMEL
Engineering Laboratory, University of Cambridge

(*Received* 19 *July* 1957)

Summary

Experiments with Perspex nozzles, which were arranged to discharge vertically downwards and in which the convergent part was followed by a short divergency, showed that at low swirls the flow was unstable. When the swirl was sufficiently large for an air core to be established, its effective magnitude was estimated from measurements, at the throat, of the core diameter and of the wall pressure. The former were in closer accord with inviscid theory than the latter. The results are presented in terms of dimensionless discharge and swirl coefficients. Measurements of core diameter and wall pressure were also made throughout one of the nozzles and compared with the theory. Reversed axial flow in the upper part of the nozzles was easily produced, and the limits of its appearance were determined. Low pressure tests with the reservoir top alternately submerged and uncovered revealed that the top had a marked influence on the nature of the flow in the nozzle; and measurements of the tangential and axial velocities in the upper part of the nozzle proved the inviscid theory to be seriously in error at high swirls. For purposes of comparison, similar experiments were performed on a convergent nozzle.

1. Introduction

In an earlier paper (Binnie & Teare 1956) an account was given of experiments on the passage of swirling water through a Perspex convergent nozzle of simple conical shape. As described below, the work has been continued with two convergent–divergent nozzles of much the same size as the nozzle previously used. The remainder of the equipment was again employed. Under these conditions a more satisfactory comparison could be made between the experiments and the inviscid theory of convergent–divergent motion, which is summarized in § 3. With the convergent nozzle it was necessary to assume that the throat lay in the plane of the nozzle outlet, but with the new nozzles the throat position was not, of course, in doubt. Moreover, better estimates of the effective swirl coefficient were possible. This coefficient cannot be reliably calculated from the wall

* On sabbatical leave from Auckland University College, New Zealand.

pressure in the convergent part of a nozzle remote from the throat because that pressure is so nearly equal to the supply head, and in a convergent nozzle the wall pressure falls rapidly to atmospheric as the outlet is approached—a state of affairs not contemplated in the theory. Thus, with more promising prospects, an attempt could now be made to determine the swirl coefficient from the throat value of the wall pressure or of the air-core diameter.

Before the new nozzles were used, for comparison some tests (described in § 4) were made on the convergent nozzle. The coreless flow that occurred at very low swirl was examined, and observations were made of the unstable conditions that set in while the air core was forming. In addition, the effect of the reservoir top on the velocity distribution in the nozzle was studied by means of low pressure tests first with the top slightly submerged and then with it slightly uncovered. In § 5 an account is given of numerous experiments on the convergent–divergent nozzles. At small swirls their action differed from that of the convergent nozzle. Under normal conditions with the core fully established, the observations at the throat of core diameter agreed much better with theory than those of wall pressure. Reverse flow was seen in the upper part of the nozzles even during high pressure tests, whereas in the convergent nozzle it occurred only at low heads. At high swirls the predictions of the inviscid theory were found very unreliable, and a detailed examination of these discrepancies was made by measuring not only the loss of total head in the nozzle but also the tangential and axial components of the velocity.

2. Description of apparatus

As shown in the upper part of figure 1, the convergent nozzle was modified by tail-pieces into alternative convergent–divergent shapes which will be designated A and B. Nozzle A was produced by attaching to the unaltered convergent nozzle a tail-piece in which the throat was a surface formed symmetrically by the revolution of a circular arc of radius 5 in. Nozzle B had a more gradual constriction, the radius of the circular arc forming the throat being 9·93 in.; before it was attached, the lower part of the convergent nozzle had to be removed. The throats of A and B were at the same level, and their diameters were respectively 0·940 and 1·088 in., the latter being identical with the throat diameter of the original convergent nozzle. The final divergent parts of both A and B were cones of semi-angle 10°, which was the same as the angle of convergence in the upper part of the nozzles.

As before, the nozzle in use was clamped to the circular base of the reservoir through an intermediate volute chamber. By this means the boundary layer formed inside the reservoir could be 'bled' off, and the maximum swirl that could be delivered to the nozzle was increased. The reservoir, which was 4 ft. 6 in. both in diameter and in height, was supplied by a vertical pipe, which entered at the centre of the top plate, and by a pair of horizontal tangential pipes. At the top of the reservoir the modification indicated in figure 1 (*d*) was made. A pipe of diameter $\frac{1}{4}$ in. was brought in to the centre of the underside of the baffle plate, and it was used to introduce air and permanganate solution and to draw off the neighbouring boundary layer. The pressures on the nozzle walls were

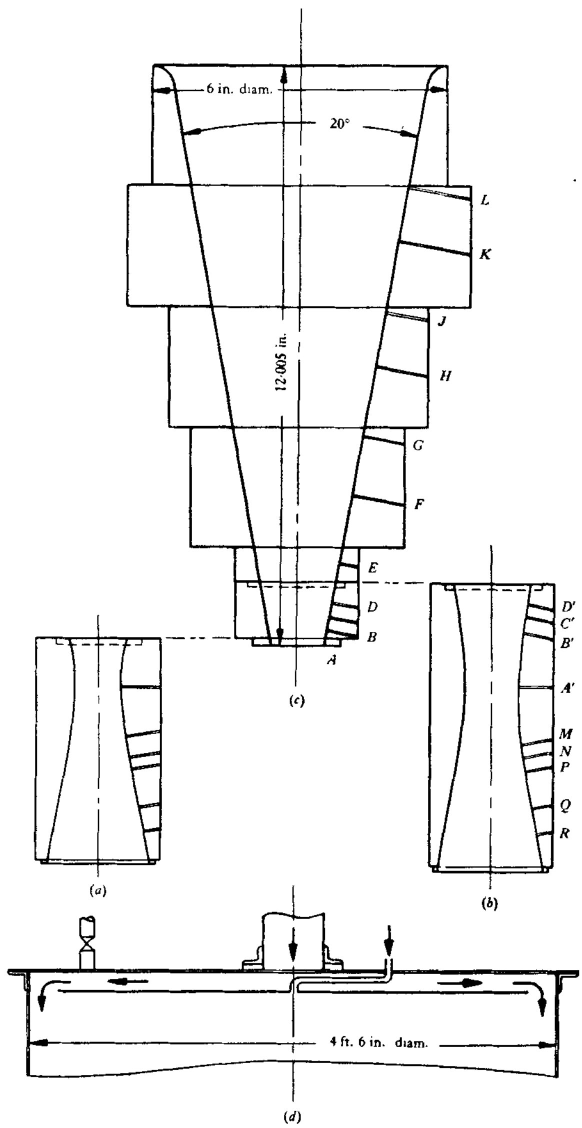

Figure 1. (*a*) tailpiece of nozzle A; (*b*) tailpiece of nozzle B; (*c*) convergent nozzle; (*d*) injection pipe at centre of baffle plate. The dimensions of nozzle B are as follows :

position	*D′*	*C′*	*B′*	*A′*	*M*	*N*	*P*	*Q*	*R*
axial distance from *L* (in.)	8·61	8·87	9·21	10·30	11·50	11·75	12·05	12·85	13·35
measured diameter (in.)	1·37	1·29	1·20	1·088	1·22	1·29	1·39	1·67	1·84

measured by tappings connected to conventional air–water and water–mercury manometers. The distribution of total head inside the nozzles was again explored through the tappings with a hypodermic tube having an outside diameter 0·027 in. and a side stagnation hole of diameter 0·014 in. Open tanks served to determine the discharge from the nozzles and the bleed. The diameter of the air core was obtained with a telescope fitted with a scale in the eyepiece but, owing to the irregular passage of waves on the core, the accuracy of these readings was not high. Refraction difficulties made this method unsatisfactory in the divergent part of the nozzle where the stream was thin, and there its radial thickness was measured with a fine wire pushed through the tappings by a micrometer screw.

3. Summary of the theory of inviscid flow

The discharge coefficient $\mathbf{K}$ and the swirl coefficient $\mathbf{X}$ are defined by

$$\mathbf{K} = \frac{\mathbf{Q}}{\pi a_t^2(2g\mathbf{H})^{1/2}}, \qquad \mathbf{X} = \frac{\Omega}{a_t(2g\mathbf{H})^{1/2}}, \tag{3.1}$$

where $\mathbf{Q}$ is the discharge, $\mathbf{H}$ is the total head of the supply measured from the level of the throat, a_t is the nozzle radius at the throat, and Ω is the swirl constant equal to the product of radius and tangential velocity. For each test $\mathbf{K}$ could be calculated from the observations of $\mathbf{Q}$ and $\mathbf{H}$, but to obtain the effective value of $\mathbf{X}$ certain relations were required which can readily be deduced from the inviscid theory explained by Binnie & Harris (1950). They are

$$\mathbf{X}^2 = \frac{1}{2}\left(1-\frac{3}{2}\frac{h_t}{\mathbf{H}}\right)\left[1 \pm \left\{1-2\frac{h_t^2}{\mathbf{H}^2}\left(1-\frac{3}{2}\frac{h_t}{\mathbf{H}}\right)^{-2}\right\}^{1/2}\right], \tag{3.2}$$

and

$$\mathbf{X}^2 = 2\frac{b_t^4}{a_t^4}\left(1+\frac{b_t^2}{a_t^2}\right)^{-1}, \tag{3.3}$$

which were used according as $\mathbf{X}$ was found from the throat wall pressure head h_t or from the core radius b_t at the throat. If the swirl is increased from a low value, $h_t/\mathbf{H}$ rises in accordance with the smaller root of (3.2) because the effect of the greater angular velocity exceeds the effect of the diminishing radial thickness of the stream. But a stage is attained when the two effects balance, and here $h_t/\mathbf{H}$ has its maximum possible value 0·343, to which the corresponding values of $\mathbf{X}$ and b_t/a_t are 0·493 and 0·644. Thereafter, since b_t increases continuously, h_t falls in accordance with the larger root of (3.2) until it reaches zero, when $\mathbf{X} = 1$, $b_t/a_t = 1$, and the discharge ceases. Thus, as Binnie & Hookings (1948) pointed out, an ambiguity arises when $\mathbf{X}$ is deduced from reading of the wall pressure, for it is impossible to distinguish between the stream with the small swirl and large radial thickness and the one with the large swirl and small thickness.

The theoretical relation between $\mathbf{K}$ and $\mathbf{X}$ may be found from (3.3) and the equation

$$\mathbf{K} = \left(1-\frac{b_t^2}{a_t^2}\right)^{3/2}\left(1+\frac{b_t^2}{a_t^2}\right)^{-1/2}, \tag{3.4}$$

the procedure being to insert in both a succession of values of b_t/a_t. The result is plotted in figures 5 and 6; it is very nearly a straight line over the range $0 < \mathbf{X} < 0{\cdot}6$. We shall also need to calculate, for specified values of $\mathbf{K}$ and for various cross-sections, the theoretical ratios of the core radius b to the nozzle radius a and of the wall pressure head h to the supply head $\mathbf{H}$. The ratio $h/\mathbf{H}$ is given by

$$\frac{h^3}{\mathbf{H}^3} - \left(1 - \mathbf{X}^2\frac{a_t^2}{a^2} - \mathbf{K}^2\frac{a_t^4}{a^4}\right)\frac{h^2}{\mathbf{H}^2} + 2\mathbf{K}^2\mathbf{X}^2\frac{a_t^6}{a^6}\frac{h}{\mathbf{H}} + \mathbf{K}^2\mathbf{X}^4\frac{a_t^8}{a^8} = 0, \qquad (3.5)$$

and then b/a is found from

$$\frac{b}{a} = \left(1 + \frac{1}{\mathbf{X}^2}\frac{a^2}{a_t^2}\frac{h}{\mathbf{H}}\right)^{-1/2}. \qquad (3.6)$$

The small difference in level between the throat and the section under consideration is here neglected; but when the calculations were carried out, the necessary correction to $\mathbf{H}$ was made. Equation (3.5) has two positive roots, the larger referring to the upstream side of the throat and the smaller to the downstream side; its last two terms were of little importance in the upper part of the nozzles where high powers of a_t/a were small.

4. Experiments on the convergent nozzle

(i) *At low swirl*

When a very small swirl was produced in the reservoir, its existence could be easily detected because, although no air core formed, the emergent jet slightly diverged. To throw light on the conditions prevailing inside the nozzle, horizontal traverses were made with the hypodermic tube inserted through a tapping. To ensure that the traverse was made across the axis of the flow, a stream of fine air bubbles was temporarily injected further upstream not far from the geometrical axis of the nozzle. The bubbles were rapidly forced to the effective axis and then discharged. In this way it was seen that usually the effective axis was distorted fairly steadily into a slightly helical shape in the same manner as an air core. Typical results of traverses extending a little way beyond the axis are plotted in figure 2, which relates to observations of total head $\mathbf{H}'$ through tappings E, F and G under constant flow conditions. When the swirl was raised as much as possible without an air core appearing, the losses of total head increased still more; and the observations followed a similar pattern to those shown in Binnie & Teare's figure 4, which were made round an air core. Again, the downward velocity near the axis was much higher than the mean. As might be expected in view of the great height of the reservoir, the loss at E was little greater than that at the higher tappings.

As the swirl was further increased, the air space within the emergent jet moved up; and when it succeeded intermittently in reaching the nozzle outlet, the flow was throttled and the reservoir pressure increased. Under these conditions readings could not be obtained. Fairly steady flow was, however, restored when a weak stream of air was injected on the axis, either at the top of the reservoir or through one of the upper tappings, causing a minute core to appear. But as soon as the injection was stopped, the air was swept out and unsteady conditions again prevailed. This device was necessary over the range $0{\cdot}92 > \mathbf{K} > 0{\cdot}78$.

The swirl being raised, a tiny air core formed of its own accord with its top darting irregularly up and down. But as it was never driven out of the nozzle and its travel was in a region where the nozzle cross-section was relatively large, the head and the discharge were not subject to appreciable fluctuations. The top of the core reached higher as the swirl was increased, until at $\mathbf{K} = 0{\cdot}64$ it was always out of sight and steady conditions were apparently established.

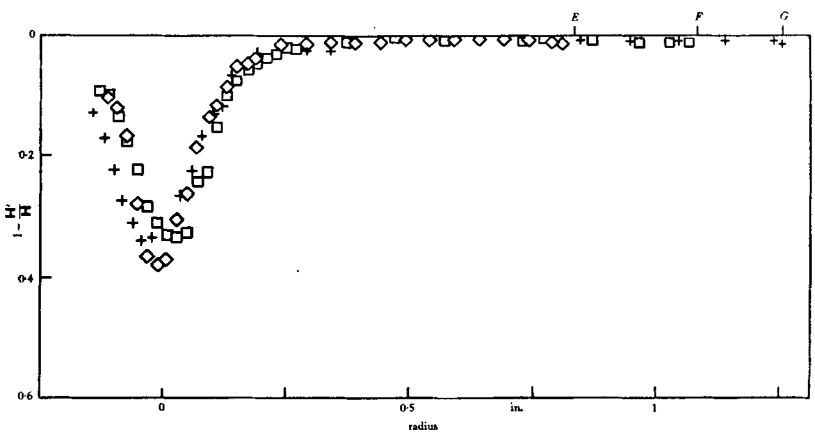

Figure 2. Fractional loss of total head in coreless flow in the convergent nozzle; + *G*; □ *F*; ◇ *E*.

The observations were continued up to the greatest available swirl, where $\mathbf{K} = 0{\cdot}48$, the final readings requiring the use of the bleed. All the above values of $\mathbf{K}$ were obtained at the constant head $\mathbf{H} = 25{\cdot}0$ ft. At $\mathbf{H} = 6{\cdot}6$ ft. the observations were unchanged except that the stage with a fluctuating self-induced core barely appeared, and the last stage occupied the range $0{\cdot}75 > \mathbf{K} > 0{\cdot}40$. No alterations in the limits were found when the tests were repeated with decreasing swirl.

(ii) *With the top of the reservoir uncovered*

To investigate the effect of the reservoir top on the flow through the nozzle, four pairs of tests were made. In the first part of each test the baffle plate (figure 1 (*d*)) was just submerged, and in the second the supply was reduced so that the baffle was just uncovered and a free surface was formed within the reservoir. In this second part, an air vent on the top plate was opened to ensure that the air pressure inside was truly atmospheric. The results of these experiments are set out in table 1 in order of diminishing swirl. Only at $\mathbf{K} = 0{\cdot}92$ was the flow coreless.

It will be seen that the submergence of the baffle plate considerably increased the discharge. In the first part, the insertion of colour through a tapping indicated a strong downward velocity close to the air core, and colour injected at the centre of the baffle was soon seen to pass through the same region. These observations confirmed Taylor's remark (1948) that the liquid, which is slowed up in the boundary layer on the back of reservoir, is unable to maintain its position, and it is quickly forced first to the core and then out through the nozzle. In the second part, there was a marked change in the appearance of the core, which was now larger in diameter and more disturbed by waves. The downward velocity near the core was greatly diminished; indeed, colour injected on the core surface was seen to move upwards an inch before being carried down by a transient train of waves.

Test	Supply	Bleed	**H** ft.	**K**
1	tangential	on	5·54 5·29	0·38 0·30
2	tangential	off	5·50 5·31	0·57 0·48
3	combined	off	5·41 5·29	0·73 0·68
4	combined	off	5·56 5·18	0·92 0·78

Table 1. The effect of a free surface inside the reservoir.

5. Experiments on the convergent-divergent nozzles

(i) *At low swirl*

The slightest introduction of swirl caused an increase in the area of contact between the stream and the divergency, and a spluttering noise was emitted, probably due to intermittent breaks in the vacuum near the throat as air from below forced its way into the zone of negative pressure. The swirl being slightly raised, the motion became quieter, and the contact between the jet and the nozzle wall was irregular (figure 3(*a*), plate 1). This state also was unstable and often reverted to the previous noisier condition. With a further increase in swirl, a loud noise was heard, and the emergent stream became wildly turbulent, drops of water being hurled out sideways with considerable velocity (figure 3(*b*), plate 1). As this highly unstable state developed, the discharge went up sharply, and the negative pressure at the throat reached its maximum value, which was about 26 ft. at **H** = 25 ft. The micro-flash photographs showed that a bubble formed with its nose at the throat and with its tail in a violent state of commotion, and it may be regarded as a cavitation bubble since the surrounding pressure was low. The admission of air through the throat tapping caused the flow to return to its previous quieter condition, but the violent state was quickly restored when the tapping was shut and the local velocity increased by the temporary insertion of a rod along the nozzle axis. At the next stage with rising swirl, the stream remained in complete contact with the whole of the divergency, but the air inside the emergent cone did not reach up above the throat. The states described in this paragraph will be referred to as phase (i). In all of them the motion was too unstable for accurate measurements to be possible. But when a small stream of air was admitted to the upper part of the nozzle, a tiny core formed exactly as described in §4(i), and steady conditions were established. Observations made in this way have been inserted in table 2.

H ft.	Test	Phase (i)	Phase (ii)	Phase (iii)
25·0	*a*	0·97–0·71	0·68–0·58	0·54–0·45
	b	0·97–0·71	0·70–0·62	0·60–0·45
6·6	*a*	0·97–0·75	—	0·71–0·41
	b	0·97–0·70	—	0·66–0·40
5·0	*a*	—	—	0·71–0·31
	b	—	—	0·68–0·31

Table 2. Values of the discharge coefficient **K** for different phases in nozzle A.

The work was continued up to the highest available swirl. In what will be termed phase (ii), a core formed intermittently above the throat but always existed near the throat itself (figure 3(*c*), plate 1), the nature of the fluctuations being the same as those observed in the convergent nozzle. Ultimately in phase (iii) a core of steady diameter was seen throughout the nozzle (figure 3(*d*), plate 1).

Table 2 gives the values of **K** obtained with the three phases in nozzle A, no great effort being made to determine with extreme precision the limits between the phases. Three supply heads were used, and with the last the reservoir top was uncovered. In the tests labelled *a* the bleed was not used at low swirls, but it required opening more and more towards the end of each test; in those labelled *b* the bleed was always fully open. This difference in the supply conditions had little effect on the results. As in the convergent nozzle, phase (ii) at **H** = 6·6 ft. made only a fleeting appearance, and no readings of it were obtained. At **H** = 5·0 ft. air injection was not tried, and attention was confined to phase (iii), which extended to much lower values of **K** than those obtained with the top of the reservoir submerged. Almost identical results were obtained with nozzle B, and the figures in table 2 agree fairly closely with those set out in §4 for the convergent nozzle.

(ii) *Comparative tests on nozzle B and the convergent nozzle*

Measurements of the core radius b and the wall pressure head h, made throughout the nozzle B at $\mathbf{H} = 24{\cdot}1$ ft., $\mathbf{Q} = 0{\cdot}111$ cu. ft./s, with the bleed discharging 0·127 cu. ft./s, are indicated by the solid points in figure 4. These conditions are almost identical with those under which the convergent nozzle had already been tested by Binnie & Teare (1956), and for purposes of comparison the observations displayed in their figure 5 have been transferred to figure 4 and plotted there as hollow points. For the above value of $\mathbf{Q}$, $\mathbf{K} = 0{\cdot}435$, the corresponding theoretical value of $\mathbf{X}$ being

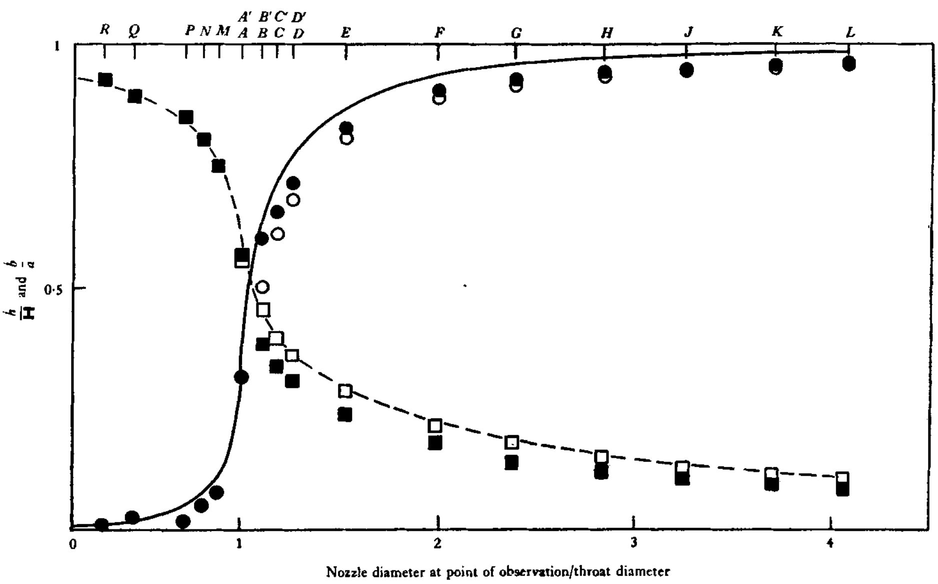

Figure 4. Core diameter and wall pressure in nozzle B.
b/a : ■ nozzle B; □ convergent nozzle; – – – theoretical relation.
$h/\mathbf{H}$: ● nozzle B; ○ convergent nozzle; ——— theoretical relation.

0·44, and the theoretical values of $h/\mathbf{H}$ and b/a are shown as curves on the diagram. As can be seen in figure 1, the throat of nozzle B was somewhat below the outlet of the convergent nozzle, which was assumed to be the effective throat. Therefore, in order that the same pair of theoretical curves might serve for both tests, the horizontal plotting in figure 4 has been done in terms of the ratio of the nozzle diameter at the point of observation to the throat diameter. Thus axial distances in the two nozzles are shown somewhat unequally in the neighbourhood of their throats. The positions of the tappings are indicated along the top of the diagram, which terminates on the left at the outlet of nozzle B.

In both tests there was fair conformity between the measured and theoretical core radii at the throat, but it must not be deduced that the flow in the nozzles closely followed the theoretical pattern. In the upper part of both, the values of h and b were less than the theoretical, and this effect may be attributed to a reduction in swirl due to viscosity. Close to the throat, the discrepancies between the pressures continued and were more noticeable in the convergent nozzle than in nozzle B. In the former the pressure fell inevitably to atmospheric, and in the latter the pressure was bound to be diminished by the curvature of the wall. The theoretical pressure curve at the throat itself is very steep, and it is difficult to judge whether or not the observation in nozzle B is in good agreement.

Observations on reversed axial flow revealed another dissimilarity between the two tests. In the convergent nozzle reverse flow was seen only at much lower supply heads. In the test on nozzle B, however, it occurred at the level of tapping K, and colour injected at J revolved horizontally with only a slight tendency to ascend. A marked difference between the flows in the two nozzles was the adverse pressure at the throat of nozzle B, and this, it seems, promoted the formation of reverse flow. This conclusion is supported by Binnie's experiments (1957) in a cylindrical tube, which showed the importance of an obstruction downstream in causing reverse flow.

(iii) *Discharge and swirl coefficients*

The values of **K** and **X** obtained in five series of tests of nozzles A and B with full bleed are plotted in figures 5 and 6. In the former, **X** was calculated by means of (3.3) from the observed core radius b_t at the throat,

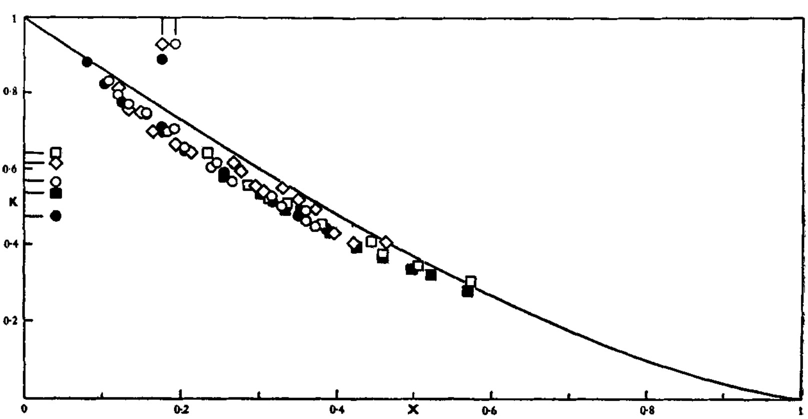

Figure 5. Observations of **K** and **X** with **X** calculated from b_t.

Head (ft.)	25·1	6·6	5·3
Nozzle A	○	◇	□
Nozzle B	●		■

——— theoretical relation.

and in the latter by means of (3.2) from the observed throat wall pressure h_t. For nozzle A, three tests were made at constant supply heads which were approximately the same as those set out in table 2, and again at the lowest head the reservoir top was uncovered. For nozzle B, tests at the intermediate head were omitted. In three of the series, observations were made at very low swirls with the aid of the air injection method described in § 4 (i), and the limits of injection are shown by the markings along the top of both figures. Reverse flow was seen in all five series, and the markings on the vertical axis of both figures indicate the limits below which reverse flow was visible. Now nozzle A had a smaller throat than B; thus reverse flow was assisted by an addition to the opposing wall pressure in the neighbourhood of the throat.

Figure 5 shows that the readings lie not far from the theoretical curve. Previous experience indicated that, in general, friction diminishes the swirl and the core radius, at the same time increasing the discharge. Thus a theoretical point is moved both to the left and upwards; and in spite of the difficulty of measuring b_t, an apparent agreement between theory and experiment was nearly obtained.

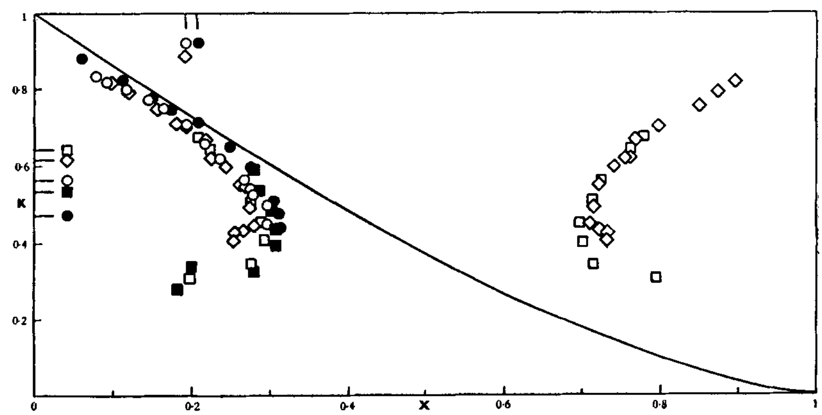

Figure 6. Observations of **K** and **X** with **X** calculated from h_t. Plotting as in figure 5.

In contrast, figure 6 reveals serious discrepancies. As already explained, (3.2) yields two possible values of **X** for each observation of h_t. The main group of points lying to the left was derived from the smaller value of **X**; for some of the same readings the larger value was calculated, and this procedure resulted in the points on the right of the diagram. It is clear that the former supposition leads to better agreement with the theoretical curve, although at the lowest values of **K**, which were attained with the reservoir top uncovered, the higher value of **X** was less distant from the theoretical curve than the lower. It will be seen that the marked departures from the theoretical curve are associated with the formation of reverse flow, and an attempt to obtain details of these discrepancies is related in the next section.

(iv) *The velocity distribution in nozzle B*

Two tests designated (*a*) and (*b*) were made with pure tangential supply and with the bleed fully open so that the swirl was the greatest obtainable. In (*a*) at **H** = 6·0 ft., **K** = 0·38, the baffle plate at the top of the reservoir was just covered, and in (*b*) at **H** = 5·3 ft., **K** = 0·28, it was just uncovered. In the former, reverse flow extended down to *G*, and in the latter to *F*. To measure the tangential velocity v in the convergent part of the nozzle a vertical rod was supported in the air core by traversing gear, which was placed below the nozzle and which enabled the rod to be centred and moved vertically. From the top of the rod a short pin protruded, round which a nylon thread about 0·006 in. thick was looped, and a small ball was attached at the other end of the thread. Contrary to expectation the ball was found to rotate without winding the thread round the rod. Its revolutions were timed with a stroboscope; and since the inclination of the thread to the horizontal was not large, the mean radius of the path of the ball was determined from the length of the thread and from a visual measurement of the vertical distance between the top of the rod and the position of the ball as it passed in front of the rod. A trial with a lead ball of diameter about 0·1 in. proved unsatisfactory, for at small immersion the tangential velocity so determined was appreciably less than that given by the light-vaned wheel shown in Binnie & Teare's figure 2(*b*) (1956). It was eventually discovered that the rod was vibrating under the centrifugal force imposed by the ball, which should have been revolving at about 5000 rev/min, and the discrepancy was almost entirely removed when the lead ball was replaced by a lighter one of bitumastic material or by a thin disc of lead. At larger radii, where the centrifugal force was less, all three particles gave the same results.

For test (*a*) at the level of tapping *H*, figure 7 shows the values of v obtained with various lengths of thread, and two observations made with the vaned wheel are also included. Near the core, v was not proportional to the radius r as it would have been had there existed a zone of appreciable thickness moving with uniform angular velocity. Actually, the tangential velocity was almost constant for about $\frac{1}{2}$ in. and then diminished towards the wall. A check on these observations was made in the following way. The radial velocity was small; and if it is neglected, integration of the radial equation of inviscid motion (Goldstein 1938, pp. 103–4) gives an expression for the wall pressure head h in the form

$$h = \frac{1}{g}\int_b^a \frac{v^2}{r}\,dr. \tag{5.1}$$

This method was applied to the curve of v and yielded $h/\mathbf{H} = 0{\cdot}89$, which is in fair agreement with the manometer reading $h/\mathbf{H} = 0{\cdot}91$ obtained at the tapping.

An endeavour was then made to estimate the distribution of the axial velocity w by measuring on photographs the inclination of a thread of colour emitted from a hypodermic tube placed at various radii. Again with neglect of the radial velocity, w was calculated from the known value

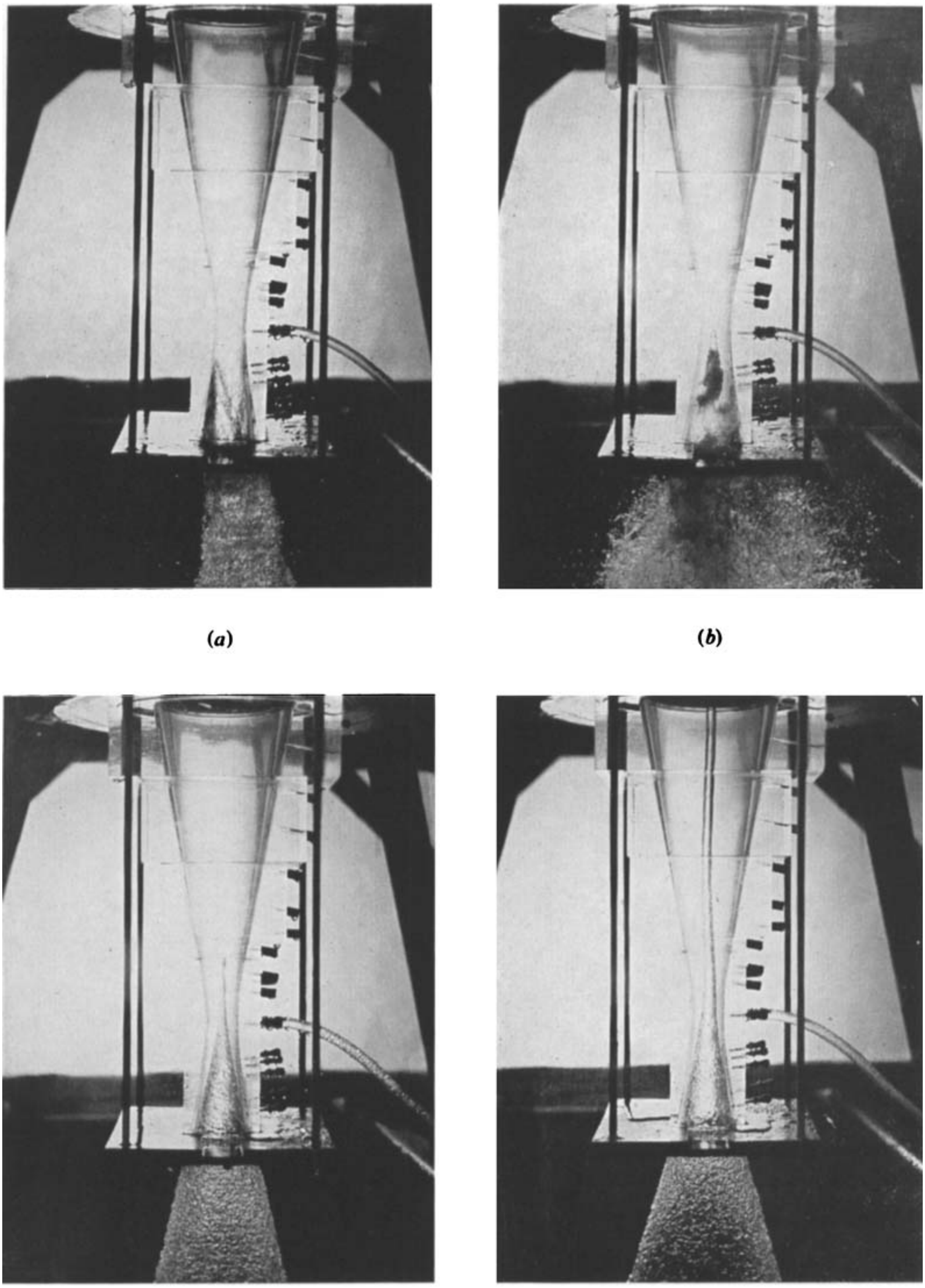

(*a*) (*b*) (*c*) (*d*)

Figure 3. Development of air core in nozzle B as swirl was increased at constant head of 25 ft.

of v in each position. The results displayed in figure 7 confirm the qualitative observations described in § 4 (ii) and indicate a large axial velocity close to the core, falling away virtually to zero in the region of reverse flow where the upward velocity was slight, and at greater radii a measurable downward velocity existed. The velocity heads due to v and w were now known, and the pressure heads were calculated by applying (5.1) to intermediate radii. The variation of loss of total head was thus determined and is shown in figure 7 by solid circles. For comparison, the

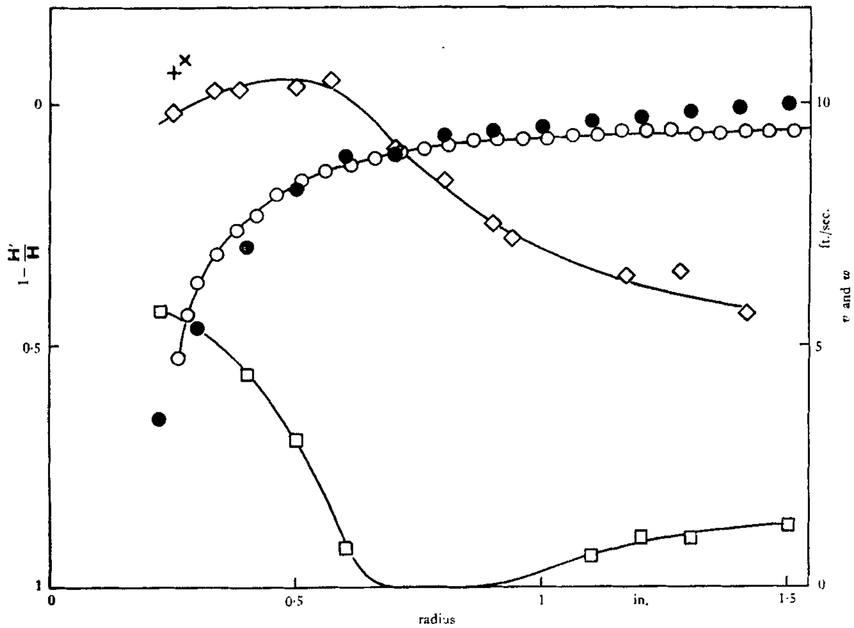

Figure 7. Velocity distribution in nozzle B with reservoir top covered. $\mathbf{H} = 6{\cdot}0$ ft.

◇ tangential velocity v measured with revolving particle.
+ tangential velocity v measured with vaned wheel 0·55 in. O.D.
× tangential velocity v measured with vaned wheel 0·65 in. O.D.
□ axial velocity w.
● fractional loss of total head calculated from observed velocities.
○ fractional loss of total head measured with total-head tube.

measurements of total head loss made directly in the manner described in § 4 (i) are shown by hollow circles. The agreement is quite good, but the method did not provide a sensitive check on the observations of w because $w^2/(2g)$ was only a minor component of the total head. A more severe test was imposed by determining the discharge $\mathbf{Q}$ from the observations of w. This yielded $\mathbf{Q} = 0{\cdot}060$ cu. ft./s, which is not in accord with the measured value 0·048 cu. ft./s. Close to the core the pitch of the helix could be measured with fair precision, but at large radii, which made important contributions to the cross-section, the streak was ill-defined and its inclination difficult to estimate; thus these latter observations were probably at fault. Nevertheless it is clear that the inviscid theory, which takes the axial velocity as uniform and the tangential velocity as varying inversely with the radius, cannot be a good approximation when the swirl is great. Similar results were found at the level of tapping F where the axial velocity was nearly but not quite reversed at a radius 0·8 in. The same checks were applied, and the agreement was somewhat better, the discharge as determined from the curve of w being 0·052 cu. ft./s. Test (*b*) failed because the core was so unstable that the $v-r$ relation could not be measured with sufficient accuracy.

It was observed that in reverse flow the injected colour moved at approximately constant radius. This is evidently due to the fact that the axial velocity w was small only in this part of the cross-section and its derivative with respect to axial distance z may be taken as zero there. A solution of the equation of continuity

$$\frac{1}{r}\frac{\partial}{\partial r}(ru) + \frac{\partial w}{\partial z} = 0 \tag{5.2}$$

is then $u = 0$.

References

Binnie, A. M. 1957 *Quart. J. Mech. Appl. Math.* **10**, 276.

Binnie, A. M. & Harris, D. P. 1950 *Quart. J. Mech. Appl. Math.* **3**, 89.

Binnie, A. M. & Hookings, G. A. 1948 *Proc. Roy. Soc.* A, **194**, 398.

Binnie, A. M. & Teare, J. D. 1956 *Proc. Roy. Soc.* A, **235**, 78.

Goldstein, S. (Ed.) 1938 *Modern Developments in Fluid Dynamics.* Oxford: Clarendon Press.

Taylor, G. I. 1948 *Proc. 7th Intern. Congr. Appl. Mech.* **2**, 280.